Dalton Transactions

Contrasting Ion-Association Behaviour of Ta and Nb Polyoxometalates

Journal:	*Dalton Transactions*
Manuscript ID:	DT-COM-08-2014-002394
Article Type:	Communication
Date Submitted by the Author:	07-Aug-2014
Complete List of Authors:	Fullmer, Lauren; Oregon State University, Chemistry Molina, Pedro; Oregon State University, Chemistry Antonio, Mark; Argonne National Laboratory, Chemistry Division Nyman, May; Oregon State University,

SCHOLARONE™
Manuscripts

Journal Name

RSC**Publishing**

COMMUNICATION

Contrasting Ion-Association Behaviour of Ta and Nb Polyoxometalates

Lauren B. Fullmer,[a] Pedro I. Molina,[a] Mark R. Antonio[b] and May Nyman*[a]

Small-angle X-ray Scattering (SAXS) studies of aqueous $[Ta_6O_{19}]^{8-}$ compared to prior studies of aqueous $[Nb_6O_{19}]^{8-}$ reveals key differences in behaviour, which is likely at the root of the difficultly in developing polyoxotantalate chemistry. Specifically, where contact ion-pairing dominates between $[Nb_6O_{19}]^{8-}$ and its counterions, solvent-separated ion-pairing between $[Ta_6O_{19}]^{8-}$ and its counterions has been unveiled in the current study.

After more than 100 years of Group V/VI polyoxometalate (POM) research, we still do not know much about the POM chemistry of Ta^V; while V^V, Mo^{VI}, W^{VI}, and now even Nb^{V} [1, 2] provide frequent exciting advances in structure,[3] solution-phase phenomena,[4] and applications.[5, 6] Ta^V is most similar to Nb^V in that clusters are formed and stable in alkaline conditions, the $[M_6O_{19}]^{8-}$ (M = Nb, Ta) Lindqvist ion dominates the solution state, they have extraordinarily high charge-density and basicity, and minimal redox activity. These PONb characteristics have been exploited in complex functional material assembly,[7] photocatalysis,[8] and base catalysis.[6] Although polyoxotantalate (POTa) science presents the greatest challenge in synthesis and isolation of well-defined species, unique discoveries in both fundamental and applied POM chemistry are the potential reward. Moreover, POTa systems are discrete, molecular counterparts to tantalate materials that have found to be exceptional photocatalysts,[9] capacitors,[10] memristors,[11] and nuclear wasteform materials.[12] To unveil and expand POTa chemistry, it is useful to delineate the differences between aqueous behavior of PONb and POTa. In this small-angle X-ray scattering (SAXS) study of $[Ta_6O_{19}]^{8-}$ in well-controlled solution conditions, we make a direct comparison of its aqueous ion-pairing behavior to that of $[Nb_6O_{19}]^{8-}$ reported prior.[13] The different behavior between the Nb and Ta analogues is surprising, given the identical structure and

charge-density. We use this concrete discovery to understand and explain recent contingent progress in POTa chemistry. The ultimate goal is to define a forward path for POTa chemistry that is intentional rather than fortuitous. Historically, the Lindqvist ion, $[Ta_6O_{19}]^{8-}$ (briefly described as a superoctahedron of six mutually edge-sharing $\{TaO_6\}$ octahedra, see figure 1) was the only known isopolyanion that forms upon aqueous (alkaline) dissolution of tantalum oxide. The structure was not presented until 1997,[14] and a reliable, completely solution-based procedure was not described until ten years later.[15] Decatantalate, $[Ta_{10}O_{28}]^{6-}$ has been very recently isolated as a tetrabutylammonium (TBA) salt from nonaqueous solution,[16] and similar chemistry was also employed to obtain TBA salts of $[H_2Ta_6O_{19}]^{6-}$.[17, 18] Even the protonated $[H_2Ta_6O_{19}]^{6-}$ clusters were a noteworthy discovery, as identification of the most basic oxo ligand of the hexatantalate cluster was under some debate.[15, 17, 19] However, unlike Nb-POM chemistry, no additional heteropolyanions, or lacunary derivatives have been observed or isolated. Meanwhile, tantalum and peroxo-tantalum substituted polyoxotungstates have recently been structurally characterized,[20] and these successes will surely lead to additional advances in the future.

In general, PONb alkali salts have a solubility trend that is opposite to that of the other polyoxometalate families,[1, 22] where solubility increases with increasing alkali countercation size; *i.e.* Li<Na<K<Rb<Cs. Prior, we took advantage of the high solubility of the
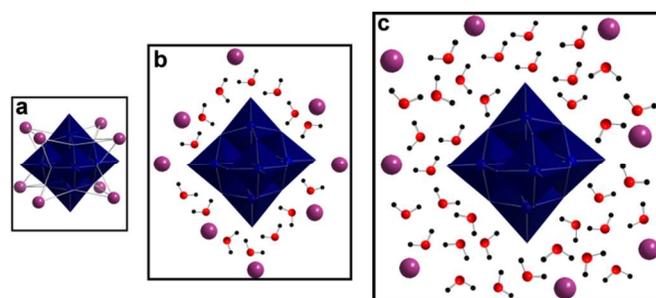
Fig. 1. Illustrating different modes of ion-pairing[21] between $[M_6O_{19}]^{8-}$ (M=Nb,Ta; blue polyhedra) and alkalis (purple spheres; K, Rb, Cs). Contact ion-pairing (a), solvent-shared ion-pairing (b) and solvent-separated ion-pairing (c).

[a] *Department of Chemistry, Oregon State University, Corvallis, OR 97331 (USA). Email: may.nyman@oregonstate.edu*

[b] *Chemical Sciences and Engineering Division, Argonne National Laboratory, Argonne, IL 60439-4831 (USA).*
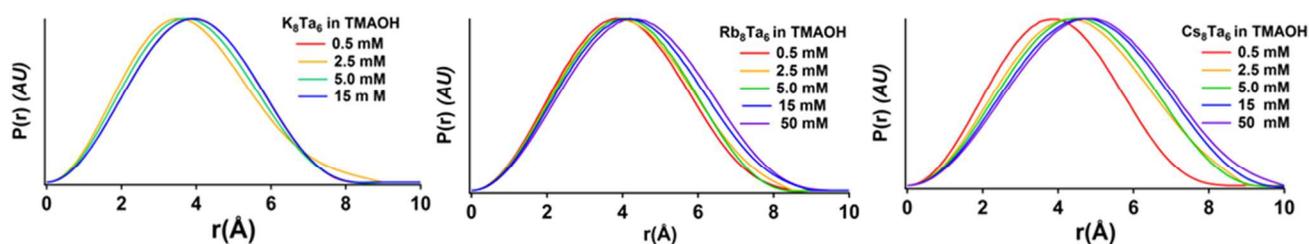
Fig. 2. Pair Distance Distribution Function (PDDF) of $[Ta_6O_{19}]^{8-}$ salts of K (left), Rb (middle), and Cs (right) in 1M TMAOH aqueous solution.

K, Rb and Cs salts of $[Nb_6O_{19}]^{8-}$ to investigate the ion-pairing between this POM anion and its alkali countercations using Small-Angle X-ray Scattering (SAXS).[13] These studies showed that in conditions of excess alkali hydroxide, the highly soluble K, Rb and Cs salts of $[Nb_6O_{19}]^{8-}$ exist in solution as a 'neutralized' species, with the alkali cations bonded directly (contact ion-pairing) to each face of the cluster—see figure 1. For the currently reported $[Ta_6O_{19}]^{8-}$ SAXS studies, we were able to achieve the same concentrations of hexatantalate salts as our prior analogous hexaniobate study,[13] approximately 0.5 to 50 mM. However, it required reducing the electrolyte [KOH, RbOH, CsOH or $N(CH_3)_4OH$ (TMAOH)] concentration from 3 to 1 molar.[23] Furthermore, the higher concentrations were challenged by apparent instability, indicated by formation of a cloudy precipitate. On the other hand, the hexaniobate solutions had seemingly limitless solubility and stability, and we were able to collect SAXS data on solutions with nearly 1M $[Nb_6O_{19}]^{8-}$ in 3M hydroxide solutions. This was our first hint that the solution states of $[Nb_6O_{19}]^{8-}$ and $[Ta_6O_{19}]^{8-}$ may in fact have noteworthy differences. Table 1 summarizes similarities and differences between the aqueous states of the Nb and Ta analogues (focusing on Rb and Cs salts), and is discussed below.

Table 1. Form factors for select (15 mM) $A_8[M_6O_{19}]$ in AOH Solutions (A=Rb,Cs, TMA; M=Nb,Ta)

	sln electrolyte	$[Nb_6O_{19}]^{8-}$		$[Ta_6O_{19}]^{8-}$	
		Rb	Cs	Rb	Cs
[1]R_g (Å)	TMA	3.1(1)	3.1(1)	2.8(4)	3.2(2)
	[3]A (Rb,Cs)	3.6(1)	3.6(1)	3.4(3)	3.8(1)
Core radius (shell radius) (Å)	[3]A (Rb,Cs)	3.9 (2.5)	4.0 (2.1)	3.8 (5.1)	4.2 (5.9)
[2]Core density (shell density) (ρ) (10^{10} cm^{-2})		58 (14)	56 (21)	134 (12)	138 (12)

[1]determined from the Guinier appoximation
[2]X-ray scattering length density (10^{10} cm^{-2}) relative to fixed solvent $\rho = 10$
[3]cluster alkali counterion(A) = electrolyte alkali(A)

The high hydroxide concentration of the solutions was strategically chosen to minimize protonation of the clusters and subsequent aggregation via mutual H-bonding of cluster faces, as has been observed in other solution conditions.[6, 24] $K_8[Ta_6O_{19}]$, $Rb_8[Ta_6O_{19}]$ and $Cs_8[Ta_6O_{19}]$ solutions in 1M TMAOH solutions have respective R_g (radius of gyration) values of 2.7(3), 2.8(4) and 3.2(2) Å, as determined by the Guinier approximation, averaged over all concentrations. The R_g values obtained from the Fourier transform method of Moore[25] agreed (see Table S1); with a distinct correlation between increasing concentration and increasing R_g and linear extent observed in the

PDDF (pair distance distribution function; see figure 2). The increase in scattering particle size with larger alkali radius and higher concentration both suggest ion-pairing is occurring, because increasing the concentration of $[Ta_6O_{19}]^{8-}$ corresponds with an 8× equivalent increase in alkali concentration. The concentration effect is particularly evident for $Cs_8[Ta_6O_{19}]$, see figure 2, consistent with the fact that larger alkalis undergo the most extensive contact ion-pairing. The R_g values, averaged over the different solution concentrations, for $A_8[Ta_6O_{19}]$ in the AOH solutions are 3.2(3), 3.4(3) and 3.8(1) Å for K, Rb and Cs, respectively. These are both bigger than the R_g values observed for those from the TMAOH solutions, and also increase with increasing alkali size. Similar to the prior $[Nb_6O_{19}]^{8-}$ studies, this too indicates ion-pairing between the alkalis and Lindqvist ion. Also like the prior studies on the analogous niobate clusters, the data was much better fit to a spherical shell model than a spherical model (see Fig SI 1-3 and Table SI1), which we would expect for a system in which the alkalis are closely associated with clusters in solution, undergoing some sort of ion-pairing. This is because the spherical shell (or core-shell) model describes the dissolved species with a bicontinuous electron density.

However, this is where the similarities between $[Nb_6O_{19}]^{8-}$ and $[Ta_6O_{19}]^{8-}$ diverge. The shape of the PDDF curves for $K_8[Nb_6O_{19}]$, $Rb_8[Nb_6O_{19}]$ and $Cs_8[Nb_6O_{19}]$ are symmetric with a radius and linear extent (figure 3) that is larger than an unassociated Lindqvist ion (4.2 and 8.4 Å respectively determined from crystal structure). These correlate in shape and size to neutralized $A_8[Nb_6O_{19}]$ specie shown in figure 1a.[13] Conversely, the PDDF plots of $A_8[Ta_6O_{19}]$ distinctly show two peaks: a larger peak at smaller radius (4.0 Å for K, 4.4 Å for Rb and 4.8 Å for Cs), with a maximum linear extent ranging from 12-16 Å; depending on concentration and identity of the alkali (figure 4). There is a general increase in radius of the first peak (and R_g) with increasing
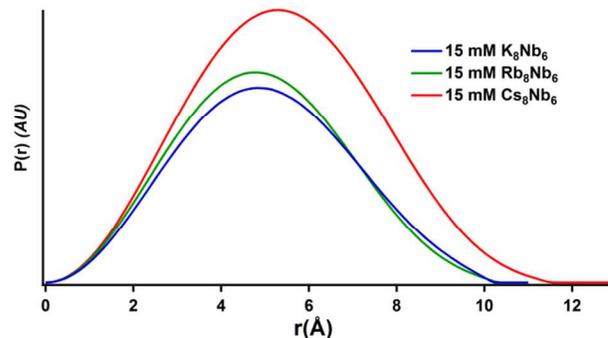

Fig. 3. PDDF of K, Rb and Cs salts of $[Nb_6O_{19}]^{8-}$ in their respective aqueous alkali hydroxide solutions indicating distinctly core-shell geometry of contact ion pairing (see also fig. 1).
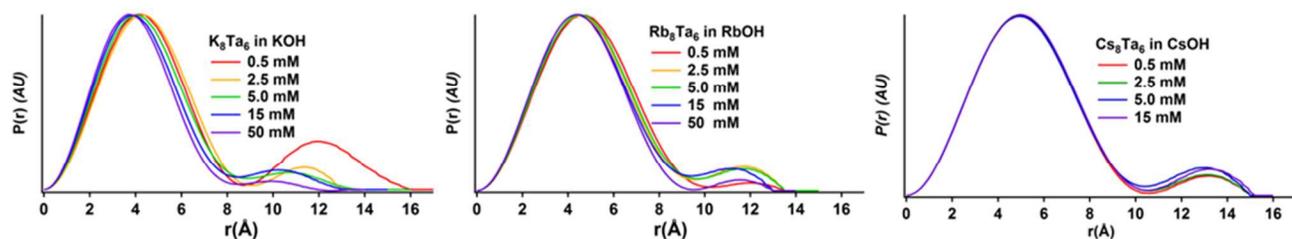
Fig. 4. PDDF of $[Ta_6O_{19}]^{8-}$ salts of K (left), Rb (middle), and Cs (right) in aqueous alkali hydroxide solutions indicating solvent-shared or solvent-separated ion-pairing (see also fig. 1), and the lowest concentration of $K_8[Ta_6O_{19}]$ suggests dimerization of the clusters via mutual hydrogen-bonding (see text).

concentration for each alkali series; suggesting some minimal contact ion-pairing occurring with Rb^+ and Cs^+ in the immediate coordination sphere of the Lindqvist ion. The second peak in these PDDF curves correlates with associated alkali-cations, separated by water molecules. The solution behavior of $K_8[Ta_6O_{19}]$ may depart from that of $Rb_8[Ta_6O_{19}]$ and $Cs_8[Ta_6O_{19}]$, based on the Moore analyses. The R_g values actually decrease with increasing concentration, see Table S1. The PDDF of the lowest concentration (figure 4) may be representative of some cluster-cluster association as has been observed prior in other solution conditions for $[Nb_6O_{19}]^{8-}$;[6] as the linear extent of both the first peak and the second peak is approximately equal to the diameter of the cluster. Since inherent ion-pairing of K is weaker than that of Rb and Cs, cluster-cluster association could compete, perhaps through mutual H-bonding of protonated faces, as suggested prior for $[H_2Nb_6O_{19}]^{6-6}$ and also for $[H_2V_{10}O_{28}]^{4-}$.[23] This would be consistent with a larger average R_g for the solution. However, as the concentration of K increases by 8× with increase in $[Ta_6O_{19}]^{8-}$ concentration, $K-[Ta_6O_{19}]^{8-}$ association becomes dominant over $[Ta_6O_{19}]^{8-}$ dimerization.

The core-shell fit to scattering curves for $Cs_8[M_6O_{19}]$ and $Rb_8[M_6O_{19}]$ (M=Nb,Ta) are compared in Table 1; and the differences correlate with those observed in the PDDFs. In these analyses, four form parameters are simultaneously fit: the electron densities of the core and shell, normalized to that of solution (fixed at $\rho=10^{10}$ cm^{-2}), and the core and shell radii. As we expect, the core radii are similar for niobate and tantalate analogues, and the electron density of the tantalate core is considerably higher than that of the niobate core. The radii of the shells for the tantalate analogues are more than 2× greater than that of the niobate analogues and they have lower electron density; which agrees with a contact ion-pairing in the niobate solutions and solvent-shared or solvent-separated ion-pairing in the tantalate solutions. This is because to shell of the tantalates include the intermediating water molecules which simultaneously increases the shell size and decreases the shell density. The core-shell fit parameters presented in Table 1 cannot quantitatively be compared directly to the PDDF parameters of figure 4. This is because the core-shell parameters take into consideration electron densities, whereas the PDDF analyses do not. However, qualitatively they represent the same concept that leads to the same conclusion.

The findings of these aqueous phase studies of $[Ta_6O_{19}]^{8-}$ compared to the prior[13] analogous studies of $[Nb_6O_{19}]^{8-}$ can be simply summarized: in high alkalinity, contact ion-pairing dominates for $[Nb_6O_{19}]^{8-}$ whereas solvent-separated or solvent-shared ion-pairing dominates for $[Ta_6O_{19}]^{8-}$. This profoundly different solution behavior is not expected, given the almost identical solid-state structures; and

furthermore suggests ion-association and acid-base chemistry of the clusters are correlated. To evaluate this point, we discuss pertinent studies below.

Prior oxo-ligand exchange studies comparing the aqueous behavior of $[H_xNb_6O_{19}]^{(8-x)-}$ to $[H_xTa_6O_{19}]^{(8-x)-}$ revealed[19, 26] one key difference related to the current study: protonated $[H_xNb_6O_{19}]^{(8-x)-}$ (x=1-3) is stable for wider pH ranges at higher pH, compared to $[H_xTa_6O_{19}]^{(8-x)-}$ (x=1-3). Moreover, solution conditions dominated by $[H_3Ta_6O_{19}]^{5-}$ were not achievable without significant decomposition of the cluster. From these reports, the niobate analogue would therefore be a stronger base.[27]

Somewhat in contrast to these studies, the solvent-separated/shared nature of the A_n-$[Ta_6O_{19}]^{n-8}$ ion-association may in fact be a result of predominant protonation of this cluster, even in high-hydroxide solution conditions. Protonation of the cluster could hinder contact ion-pairing in two ways: 1) by reducing the charge-density on the cluster thus decreasing the attraction to alkalis and 2) by occupying coordination sites on the clusters' basic oxo ligands that could otherwise bond to an alkali cation. This behavior would suggest the hexatantalate is a stronger base than hexaniobate, inconsistent with prior characterization in solution. However, the prior solution studies only accounted for intact clusters remaining in solution; it is possible, even probable, that hydrated tantalum oxide/hydroxide forms and precipitates as a result of even slight acidification in water. High basicity and resultant reactivity of purely tantalate clusters could also explain why 1) aqueous solutions of alkali hexatantalate eventually precipitate out hydrous tantalum oxide, even in 1 molar hydroxide; and 2) tantalate POMs other than $[Ta_6O_{19}]^{8-}$ or tantalate cores capped by tungstate lacunary fragments[20] have not yet been isolated from water.

Finally, we come to the relationship between differing ion-pairing behavior observed, under the experimental conditions of this study, and the distinctly lower solubility of $[Ta_6O_{19}]^{8-}$ compared to $[Nb_6O_{19}]^{8-}$, a relationship which too can be rationalized. Considering the ion-pairing of $[Nb_6O_{19}]^{8-}$, it essentially exists as a neutralized species in the AOH (A = K, Rb, Cs) solutions. The close association between the alkalis and the cluster anion may suggest that the ion-paired Cs-cations do not necessitate bridging to other anionic clusters or even strongly bonding to water in order to satisfy bond valence. A resultant lack of attraction between the neutral $Cs_8[Nb_6O_{19}]$ species could then explain its high solubility. By contrast, the hydration sphere between $[Ta_6O_{19}]^{8-}$ and its alkali counterions prevents close association, so these alkalis can bridge two or more clusters to satisfy bond valence, a solution state that results in precipitation. However, $[Ta_6O_{19}]^{8-}$ like $[Nb_6O_{19}]^{8-}$ does exhibit an anomalous solubility trend

compared to other POMs where the Cs-salts are more soluble than Li-salts; suggesting that the solvent-separated ion association of $A_8[Ta_6O_{19}]$ still has strong electrostatic association between the alkalis and the anionic cluster.

In this study we have directly observed solvent-separated and/or solvent-shared ion-association of the hexatantalate POM, in contrast to the contact ion-association of isostructural hexaniobate. Since hexatantalate is the only recognized stable Ta-POM specie in water, these findings provide an insight into why aqueous Ta-POM chemistry remains elusive; and advances have only come from nonaqueous conditions. The observation of solvent-separated/solvent-shared ion-association along with other circumstantial evidence leads to the hypothesis that the inevitable protonation of the highly-charged Ta-POMs in water results in decomposition. More than a century of ongoing POM research has revealed that despite structural similarities between Group V and Group VI POMs, aqueous behaviour differs vastly including pH of self-assembly and stability, and solubility trends. This study brings forth yet another distinction of opposing behaviour between Group V and Group VI. In Group VI POMs, the heavier congener W is stable to rearrangement in solution with varying pH; whereas Mo POMs famously are labile in solution resulting in the well-known giant molybdate capsules. Here we recognize the heavier congener of the Group V POMs exhibits greater instability in solution. However, unlike molybdate, the lack of a stable monomer inhibits exploiting this characteristic to isolate other Ta-POMs from water. Thus the promising path forward for Ta-POM chemistry, as revealed by recent studies, is via non-aqueous routes.

Notes and references

1   M. Nyman and P. C. Burns, Chem Soc Rev, 2012, 41, 7354. M. Nyman, *Dalton Trans.*, 2011, **40**, 8049.
2   Y. Zhang, J. Q. Shen, L. H. Zheng, Z. M. Zhang, Y. X. Li and E. B. Wang, *Cryst. Growth Des.*, 2014, **14**, 110; C. A. Ohlin, E. M. Villa, J. C. Fettinger and W. H. Casey, *Inorg. Chim. Acta*, 2010, **363**, 4405; J. H. Son, C. A. Ohlin, R. L. Johnson, P. Yu and W. H. Casey, *Chem. Eur. J.*, 2013, **19**, 5191; J. H. Son, J. Wang, F. E. Osterloh, P. Yu and W. H. Casey, *Chem. Commun.*, 2014, **50**, 836.
3   A. Müller and P. Gouzerh, *Chem. Soc. Rev.*, 2012, **41**, 7431; O. Oms, A. Dolbecq and P. Mialane, *Chem. Soc. Rev.*, 2012, **41**, 7497; H. J. Lv, Y. V. Geletii, C. C. Zhao, J. W. Vickers, G. B. Zhu, Z. Luo, J. Song, T. Q. Lian, D. G. Musaev and C. L. Hill, *Chem. Soc. Rev.*, 2012, **41**, 7572.
4   P. C. Yin, D. Li and T. B. Liu, *Chem. Soc. Rev.*, 2012, **41**, 7368; Y. Hou, L. N. Zakharov and M. Nyman, *J. Am. Chem. Soc.*, 2013, **135**, 16651.
5   J. M. Clemente-Juan, E. Coronado and A. Gaita-Ariño, *Chem. Soc. Rev.*, 2012, **41**, 7464.
6   M. K. Kinnan, W. R. Creasy, L. B. Fullmer, H. L. Schreuder-Gibson and M. Nyman, *Eur. J. Inorg. Chem.*, 2014, **2014**, 2318.
7   M. Nyman, A. J. Celestian, J. B. Parise, G. P. Holland and T. M. Alam, *Inorg. Chem.*, 2006, **45**, 1043; M. Nyman, F. Bonhomme, T. M. Alam, M. A. Rodriguez, B. R. Cherry, J. L. Krumhansl, T. M. Nenoff and A. M. Sattler, *Science*, 2002, **297**, 996.
8   J. Q. Shen, Y. Zhang, Z. M. Zhang, Y. G. Li, Y. Q. Gao and E. B. Wang, *Chem. Commun.*, 2014, **50**, 6017; P. Huang, C. Qin, Z. M. Su, Y. Xing, X. L. Wang, K. Z. Shao, Y. Q. Lan and E. B. Wang, *J. Am. Chem. Soc.*, 2012, **134**, 14004.
9   H. Kato and A. Kudo, *Catal. Today*, 2003, 78, 561; F. E. Osterloh, *Chem. Mater.*, 2008, **20**, 35; H. Kato and A. Kudo, *J. Phys. Chem. B*, 2001, **105**, 4285; A. Yamakata, T. Ishibashi, H. Kato, A. Kudo and H. Onishi, *J. Phys. Chem. B*, 2003, **107**, 14383.
10 C. Chaneliere, J. L. Autran, R. A. B. Devine and B. Balland, *Mat. Sci. Eng. R.*, 1998, **22**, 269.
11 J. P. Strachan, G. Medeiros-Ribeiro, J. J. Yang, M. X. Zhang, F. Miao, I. Goldfarb, M. Holt, V. Rose and R. S. Williams, *Appl. Phys. Lett.*, 2011, **98**, 241114.
12 F. X. Zhang, M. Lang, J. M. Zhang, R. C. Ewing and M. Nyman, *J. Solid State Chem.*, 2011, **184**, 2329.
13 M. R. Antonio, M. Nyman and T. M. Anderson, *Angew. Chem. Int. Ed.*, 2009, **48**, 6136.
14 H. Hartl, F. Pickhard, F. Emmerling and C. Rohr, *Z. Anorg. Allg. Chem.*, 2001, **627**, 2630. F. Pickhard and H. Hartl, *Z. Anorg. Allg. Chem.*, 1997, **623**, 1311.
15 T. M. Anderson, M. A. Rodriguez, F. Bonhomme, J. N. Bixler, T. M. Alam and M. Nyman, *Dalton Trans.*, 2007, 4517.
16 M. Matsumoto, Y. Ozawa, A. Yagasaki and Y. Zhe, *Inorg. Chem.*, 2013, **52**, 7825.
17 M. Matsumoto, Y. Ozawa and A. Yagasaki, *Inorg. Chem. Comm.*, 2011, **14**, 115.
18 M. Matsumoto, Y. Ozawa and A. Yagasaki, *Inorg. Chem.*, 2012, **51**, 5991.
19 E. Balogh, T. M. Anderson, J. R. Rustad, M. Nyman and W. H. Casey, *Inorg. Chem.*, 2007, **46**, 7032.
20 S. Li, S. Liu, S. Liu, Y. Liu, Q. Tang, Z. Shi, S. Ouyang and J. Ye, *J. Am. Chem. Soc.*, 2012, **134**, 19716.
21 Y. Marcus and G. Hefter, *Chem. Rev.*, 2006, **106**, 4585.
22 Y. Hou, M. Nyman and M. A. Rodriguez, *Angew. Chem. Int. Ed.*, 2011, **50**, 12514.
23 To confirm the differences we observe in $[M_6O_{19}]^{8-}$ (M=Nb,Ta) SAXS studies are a result of Nb vs. Ta and not the molarity of the hydroxide, select SAXS data were collected on $[Nb_6O_{19}]^{8-}$ salts in 1M hydroxide solutions. These point checks confirmed that the concentration of the hydroxide did not affect the solution ion-association.
24 T. Kojima, M. R. Antonio and T. Ozeki, *J. Am. Chem. Soc.*, 2011, **133**, 7248.
25 P. B. Moore, *J. Appl. Crystallogr.*, 1980, **13**, 168.
26 J. R. Black, M. Nyman and W. H. Casey, *J. Am. Chem. Soc.*, 2006, **128**, 14712.
27 In agreement, mono-, di- and triprotonated hexaniobate (M. Nyman, T. M. Alam, F. Bonhomme, M. A. Rodriguez, C. S. Frazer and M. E. Welk, *J. Cluster Sci.*, 2006, **17**, 197) have been isolated in the solid-state from water, but isolation of a protonated hexatantalate from water has never been documented. The isostructural sodium salts of $[Nb_6O_{19}]^{8-}$, the original Lindqvist ion (I. Lindqvist, *Arkiv Kemi*, 1953, **5**, 247) and $[Ta_6O_{19}]^{8-}$ provide a specific example where a direct comparison can be made. The niobate analogue is monoprotonated, whereas the tantalate analogue is not protonated: rather it has an extra sodium occupying a lattice position that is identified as water in the niobate analogue (T. M. Anderson, M. A. Rodriguez, F. Bonhomme, J. N. Bixler, T. M. Alam and M. Nyman, *Dalton Trans.*, 2007, 4517).

Table of contents graphic